

Understanding Changes in the Asian Summer Monsoon over the Past Millennium: Insights from a Long-Term Coupled Model Simulation*

FANGXING FAN AND MICHAEL E. MANN

Department of Meteorology, and Earth and Environmental Systems Institute, The Pennsylvania State University, University Park, Pennsylvania

CASPAR M. AMMANN

Climate Global Dynamics Division, National Center for Atmospheric Research, Boulder, Colorado

(Manuscript received 20 November 2007, in final form 4 September 2008)

ABSTRACT

The Asian summer monsoon (ASM) and its variability were investigated over the past millennium through the analysis of a long-term simulation of the NCAR Climate System Model, version 1.4 (CSM 1.4) coupled model driven with estimated natural and anthropogenic radiative forcing during the period 850–1999. Analysis of the simulation results indicates that certain previously proposed mechanisms, such as warmer large-scale temperatures favoring a stronger monsoon through their effect on Eurasian snow cover, appear inconsistent with the mechanisms active in the simulation. Forced changes in tropical Pacific sea surface temperatures play an apparent role in the long-term changes in the ASM. Analyses of the simulation results suggest that the direct radiative effect of solar forcing variations on the ASM is quite weak and that dynamical responses may be far more important. Volcanic radiative forcing leads to a clearly detectable short-term reduction in the strength of the ASM. Comparisons with long-term proxy reconstructions of the ASM are attempted but are limited by the divergent behavior among different reconstructions as well as the limitations in the model's coupled dynamics.

1. Introduction

The Asian monsoon is associated with changes in the large-scale atmospheric circulation over substantial parts of Asia. These changes are driven by the differential seasonal diabatic heating of the Asian continent and tropical Indo-Pacific Ocean. The boreal summer phase of the monsoon is associated with surface convergence of moisture, and hence precipitation, over large parts of South and Southeast Asia. Given the effects on water resources over these densely populated regions, it is of considerable importance to understand the possible future effects of climate change on the Asian

summer monsoon (henceforth ASM; e.g., Meehl and Arblaster 2003; Meehl et al. 2007).

A simple view has been that anthropogenic greenhouse warming is likely to strengthen the ASM as a result of the differential warming of land and ocean that arises from the delay in ocean surface warming. All other factors being equal, greater warming over land-masses implies greater land–sea heating contrasts, in turn favoring a stronger summer monsoon. It has also been suggested that decreased spring and early summer snow cover over the Eurasian continent associated with warming temperatures, by decreasing the energy consumed for snowmelt, may increase the energy available for driving the summer monsoon (Barnett et al. 1989; Meehl 1994). However, there are numerous other factors that could actually offset or even reverse this response. Increased atmospheric water vapor content (i.e., specific humidity) associated with a warmer tropical atmosphere is likely to increase monsoon-related precipitation, and thus the midtropospheric latent heating. This increased latent heating tends to stabilize the atmosphere, inhibiting the vertical convective heat transport

* Supplemental information related to this paper is available at the Journals Online Web site: <http://dx.doi.org/10.1175/2008JCLI2336.s1>.

Corresponding author address: Fangxing Fan, Department of Meteorology, The Pennsylvania State University, 408 Walker Building, University Park, PA 16802.
E-mail: fxf908@psu.edu

that maintains the mean thermally driven circulation. Counterintuitively, the mean monsoonal circulation is thus projected to weaken even as the monsoon-related precipitation itself increases [see, e.g., Meehl et al. (2007) and references therein]. Increased tropospheric aerosols (aside from absorbing aerosols, such as black carbon) may also have a countering effect, since they reduce the received surface shortwave radiation and hence the differential summer heating of land and ocean. Yet, the precise magnitude of anthropogenic aerosol forcing remains uncertain.

There are additional complications in projecting how the ASM will respond to future climate forcing related to climate dynamics. The El Niño–Southern Oscillation (ENSO) affects the monsoon by altering the zonal pattern of moisture transport in the Indo-Pacific connected with the Walker circulation (see, e.g., Nigam 1994; Webster et al. 1998). Indeed, substantial historical monsoon failures have been identified with strong El Niño events (Grove 1998). Effects of climate change on ENSO itself may influence future changes in the monsoon (see Krishna Kumar et al. 1999, 2006). Current limitations in our ability to project changes in the mean state and variability of the tropical Pacific coupled ocean–atmosphere system (Meehl et al. 2007) therefore translate to uncertainties in our ability to project changes in the ASM.

Given the profound potential future impacts on society of changes in the ASM, there is good reason to strive for a better understanding of possible future changes. One approach is to study past variations in the monsoon and attempt to determine their causes. In this study, we pursue such an investigation. We apply a new method for defining an index of the ASM to the analysis of a long-term simulation [National Center for Atmospheric Research (NCAR) Climate System Model, version 1.4 (CSM1.4) coupled model] of the climate of the past millennium. In the context of the simulation, the changes in both natural and anthropogenic forcing are precisely known (i.e., they are exactly as specified in the model) and their effect on the monsoon can be diagnosed. We interpret proxy and historical evidence for past changes in ASM in the context of this analysis.

2. Defining an index of the Asian summer monsoon

Given that distinct subsystems of the ASM, in particular the South Asian and East Asian monsoons, experience different dynamical influences, it is likely that these subsystems will exhibit different patterns of internal and externally forced variability. We, therefore, performed separate analyses for the broadly defined ASM (40°–180°E, 0–60°N) and both the “South Asian” (40°–

105°E, 0–60°N) and “East Asian” (105°–180°E, 0–60°N) monsoon subsystems (henceforth referred to as SASM and EASM, respectively).

We employed a newly developed approach to define indices of the monsoon. This approach employs a principal component analysis (PCA) dimensional reduction procedure to isolate the common pattern of variation among three fields—sea level pressure (SLP), zonal wind shear ($U_{850} - U_{200}$), and meridional wind shear ($V_{850} - V_{200}$)—which characterize the boreal summer atmospheric circulation over the region defining the monsoon (see, e.g., Webster and Yang 1992; Goswami et al. 1999). For the SLP and $U_{850} - U_{200}$ fields, where there is typically a single dominant pattern, we retained only the leading empirical eigenvector, that is, the leading principal component (PC) and empirical orthogonal function (EOF). For $V_{850} - V_{200}$, the first two eigenvectors were typically observed to be degenerate or nearly so (see, e.g., S1 of the online supplement), thus both eigenvectors were retained. The dominant patterns of variation in the three fields were accordingly defined by the multivariate dataset consisting of these four eigenvectors.

Monsoon-related precipitation—for example, all-India monsoon rainfall (AIMR; see Parthasarathy et al. 1992)—has also been used as an index of the ASM. Given the potential decoupling between monsoon-related precipitation and monsoonal circulation strength in a changing climate as discussed above, we have chosen to define a monsoon index independently from the precipitation field and diagnose any potential relationships between our circulation-based monsoon index and the precipitation field subsequently.

An integrative monsoon index (IMI) was defined as the leading PC series of the multivariate dataset constituted by the four PC series discussed above (each normalized to have unit variance), representing the three fields (SLP, zonal wind shear, and meridional wind shear) over the associated spatial domain. Our procedure for defining a multivariate monsoon index is in certain respects similar to that used by Wolter and Timlin (1993) to define a multivariate ENSO index in terms of a group of atmospheric and oceanic variables influenced by ENSO. Further details, including applications of the procedure to the behavior of NCAR CSM1.4 simulation and NCEP reanalysis during the last half century, are provided in the online supplement (see S1). Application of our procedure to NCEP reanalysis data gives similar results to standard climatology-based measures of the monsoon (S2 of the online supplement). In fact, the resulting SASM IMI is on average more highly correlated with three existing SASM measures (Webster and Yang 1992; Goswami et al. 1999; Parthasarathy et al. 1992)

than they are with each other (see S2 of the online supplement). A key strength of our methodology, however, is that it is tied to the variability, rather than climatology, of the underlying atmospheric fields. For this reason, the methodology can be readily applied to the characterization of monsoonal behavior in model simulations whose climatological features differ from those of the actual climate. Such an application is described below with respect to a long-term simulation of the NCAR CSM1.4 coupled model.

3. Application to model simulation

We wish to use the methodology outlined in section 2 to characterize the behavior of the ASM in a long-term forced simulation of the NCAR CSM1.4, which is a global coupled atmosphere–ocean–sea ice–land surface model with no flux adjustments (Boville and Gent 1998; Boville et al. 2001; Otto-Bliesner and Brady 2001). In the simulation analyzed here, the model was forced over the period 850–1999 with estimated natural forcing from solar irradiance and volcanic aerosols, and anthropogenic forcing as a result of changes in greenhouse gases and anthropogenic sulfate aerosols. Also included is an annual cycle of ozone and natural sulfate aerosol. A detailed description of the model simulation and forcings used is provided by Ammann et al. (2007).

We performed separate analyses as described above to characterize the ASM, SASM, and EASM in the NCAR CSM1.4 simulation. The model simulation provided a structurally faithful reproduction of the real world SASM, as represented in a parallel analysis of NCEP reanalysis data (see S1 of the online supplement). The key SLP pattern features—including the broad low pressure over tropical South Asia and, in particular, the deep trough over the Himalayan plateau—are reproduced in the simulation, as is the north–south dipole structure in the zonal wind shear field (see Fig. 1). The leading pattern of meridional wind shear, characterized by a zonal tripolar structure, is reproduced as well, though it appears—in the case of the model simulation—as the secondary of the degenerate first two leading wind shear modes.

By contrast, the EASM (and by extension, the eastern-most features of the broadly defined ASM) were found to be poorly reproduced by the model (see S3 of the online supplement), resulting in large part from the model's inability to reproduce important features of the tropical Pacific intertropical convergence zone (e.g., the “split ITCZ” bias common to essentially all coupled models; see Kiehl 1998). We, therefore, chose to focus the foregoing analysis of the model monsoon behavior

on the SASM, for which we believe any inferences from the simulation are most likely to be meaningful.

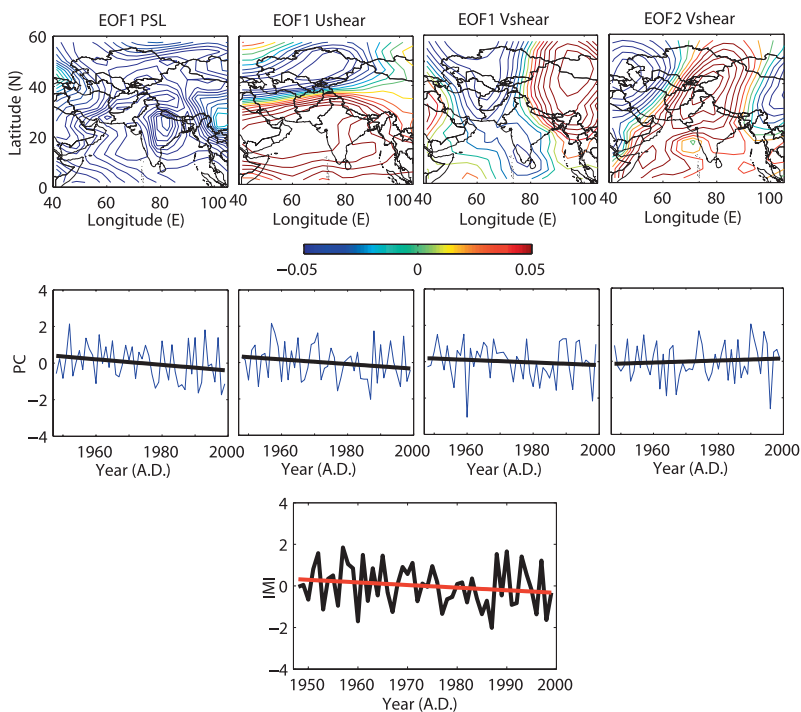
There is also some qualitative similarity between the model and NCEP observations in the behavior of the SASM during the late twentieth century. In both cases (see Fig. 1), there is a decreasing trend in the strength of the SASM during this time interval. Although the trend is far more pronounced in the reanalysis data than in the NCAR simulation, the documented potential for spurious long-term trends in the reanalysis data (e.g., Hurrell and Trenberth 1998) requires that trends in the former be interpreted cautiously. The weakening trend in the NCEP reanalysis is, nonetheless, at least qualitatively consistent with certain factors discussed earlier—that is, the increased midtropospheric latent heating as a result of increased specific humidity associated with a warming atmosphere and the effect of anthropogenic sulfate aerosol forcing. In the longer-term context provided by the simulation, this trend is indeed observed to be anomalous in the context of the entire millennial-long simulation.

Application of our analysis to the entire simulation (Fig. 2) reveals an anomalous weakening of the monsoon in the twentieth century, which is reflected in each of the three underlying fields (In the case of meridional wind shear, the trend is expressed in the second PC series; note that the order of the first two EOFs–PCs switches in the full period analysis relative to the late twentieth century analysis shown in Fig. 1). Interestingly, the anomalous trend is not observed in the leading EOF–PC of the precipitation field over the SASM region (Fig. 3). The precipitation pattern is highly correlated with the IMI at both annual (0.59; see section S1 of the online supplement) and decadal (0.39; see Table 1) time scales, but the late twentieth century trend is absent in the precipitation pattern. This observation is consistent with the potential decoupling of monsoon circulation strength and monsoon precipitation in a warming climate discussed earlier.

4. Comparisons with proxy evidence

Several quantitative reconstructions of the SASM have been attempted with climate proxy data. We have compared four such reconstructions (Fig. 4a) with our monsoon index. Each reconstruction has been standardized to have the same multidecadal variance as the model-based SASM IMI, and each has been defined to be positive (negative) for an inferred stronger (weaker) monsoon. The reconstructions include the following: (i) Wang et al. (2005), who attempted to reconstruct changes in monsoon intensity using a speleothem oxygen isotope record from southern China that reflects changes

a) NCAR CSM 1.4 (1948-1999)



b) NCEP (1948-2000)

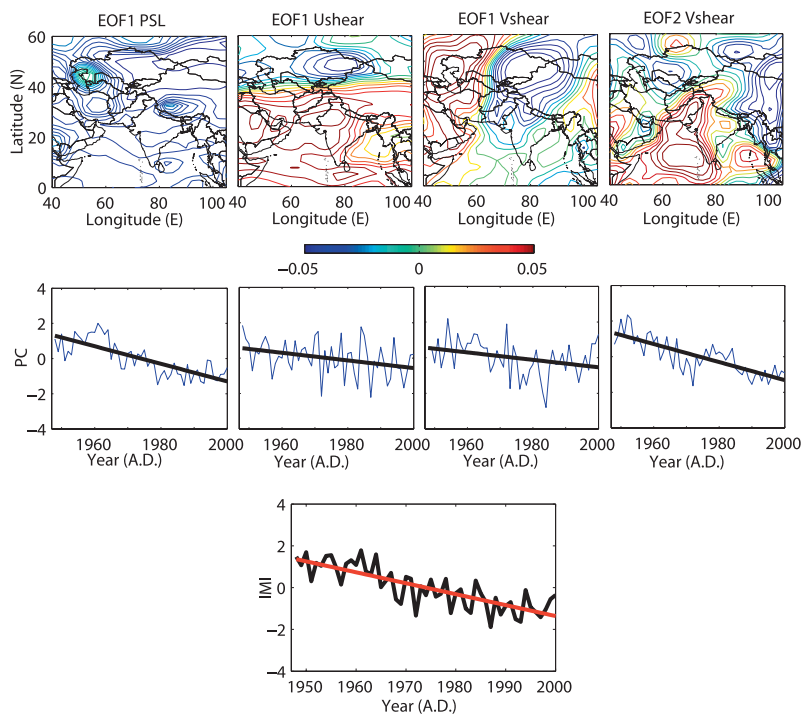


FIG. 1. EOF patterns of (top) (left to right) EOF1 SLP and zonal wind shear and EOF1 and 2 meridional wind shear; (middle) corresponding PC series; and (bottom) resulting IMI series over SASM spatial domain for (a) NCAR CSM1.4 simulation 1948–99 and (b) NCEP reanalysis 1948–2000.

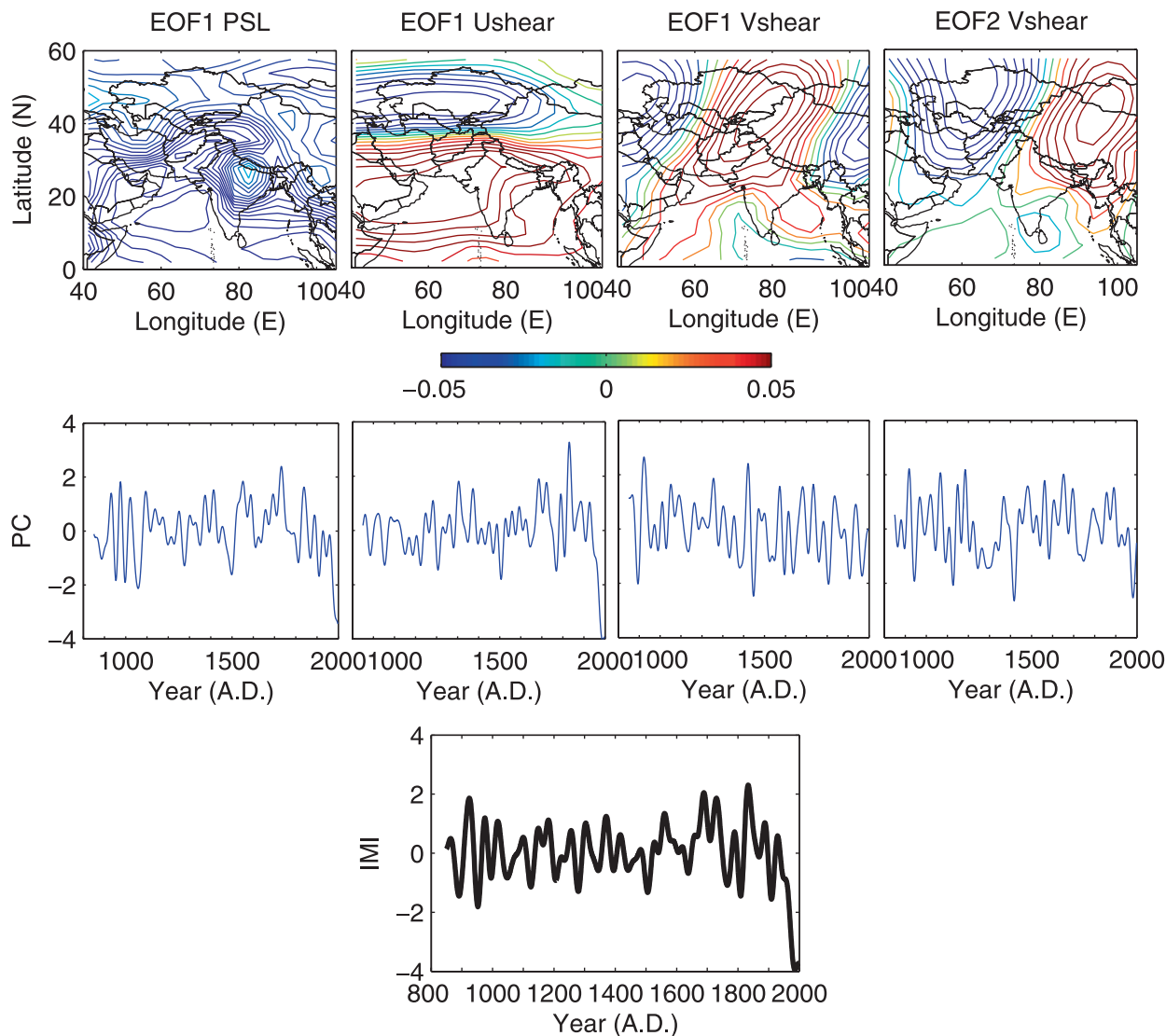


FIG. 2. Analysis of SASM behavior in NCAR CSM1.4 simulation 850–1999. Shown are EOF patterns, PC series, and IMI series as in Fig. 1, but during the period 850–1999. Here, as in all similar figures below, time series have been smoothed on multidecadal time scales, based on a low-pass filter designed to retain variability on time scales greater than 33 yr (see Mann 2004).

in moisture in the region. [As evident from a comparison with NCEP reanalysis data (Fig. 4b), monsoon strength is expected to vary inversely with summer precipitation in this region.] (ii) Anderson et al. (2002), who used a wind-driven upwelling proxy (*G. bulloides* foraminiferal abundance), measured in an ocean sediment core from the northwestern Arabian Sea to infer long-term changes in what they refer to as the Asian “southwest” monsoon [A positive relationship between monsoon strength and alongshore winds near the site of the record is evident (Fig. 4b)]. (iii) Thompson et al. (2000) inferred changes in the ASM from an ice core dust record that is negatively correlated with summer precipitation over the Tibetan Plateau (and hence, the strength of the SASM) based on

its relationship with modern instrumental precipitation data. [They note, for example, that certain features of the record (e.g., the inferred major monsoon failure between 1790–96) are consistent with the known negative affect of El Niño events on summer monsoon failure. The inferred negative relationship with local precipitation is consistent with modern reanalysis data (Fig. 4b).] (iv) Cook and Krusic (2009) similarly infer Indian monsoon strength from its inverse relationship with drought sensitive tree-ring data from the Tibetan Plateau.

Comparisons between our model-based SASM IMI series with the various proxy reconstructions yield limited agreement (Fig. 4). Only two (1 and 2) of the three proxy reconstructions are significantly (i.e., at the positive

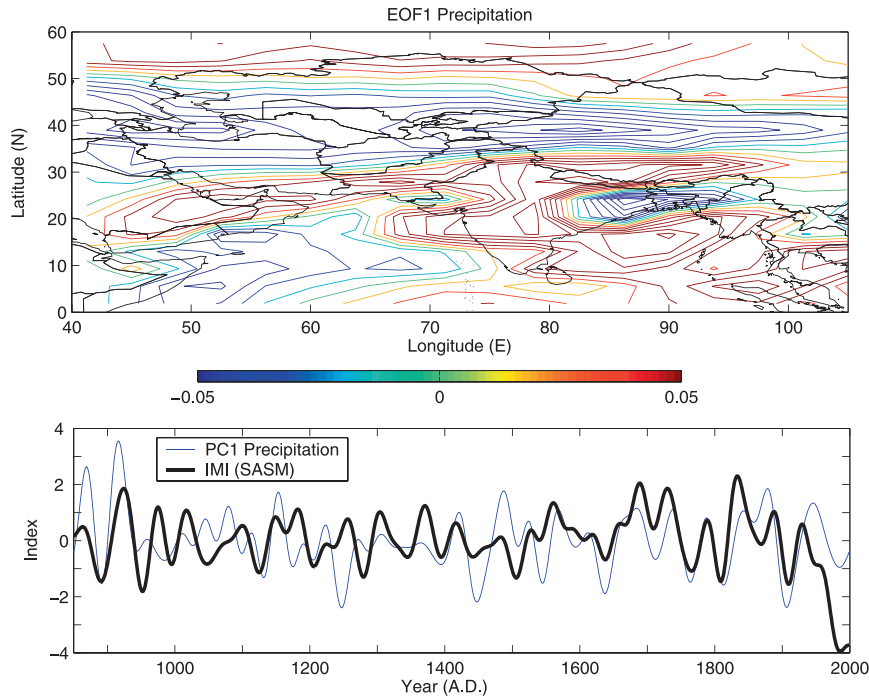


FIG. 3. Analysis of long-term SASM precipitation variations in NCAR CSM1.4 simulation 850–1999. Shown is (top) leading EOF of precipitation field during the period 850–1999 and (bottom) corresponding PC. Precipitation PC is shown along with the IMI series of Fig. 2 for comparison.

$p = 0.01$ level) correlated with each other (Table 2) at multidecadal time scales, indicating that there is significant uncertainty in the proxy reconstructions of past monsoon behavior themselves. On multidecadal time scales where external forcing might be expected to dominate the behavior of the SASM, there is an only marginally significant relationship ($p < 0.1$) with just one of the four reconstructions (the Dasuopo ice core dust record; see Table 2), and this arises from the fact that the reconstruction, like the model, indicates a substantially weakening SASM during the twentieth century. If the twentieth century is eliminated, then the same reconstruction no longer exhibits a positive correlation with the model IMI series and instead an entirely different proxy—the Arabian sea upwelling proxy record (Table 2)—exhibits a marginally significant positive correlation with the model IMI series. Yet, this reconstruction exhibits a substantial positive trend in late-nineteenth and twentieth centuries that is contrary to the negative trend seen in the model-based monsoon index, and the correlation over the full period of overlap is negative. As discussed earlier, modern observations indicate a statistically significant decline in the strength of the SASM during the latter half of the twentieth century that is in agreement with the negative late twentieth-

century trend evident in the model-based IMI. Yet, in two of the three proxy reconstructions (1 and 2), the late twentieth-century trend is strongly positive, contradicting the observations.

Clearly, the inferred long-term changes in the Asian monsoon during the past 1000 yr are not consistent between the different proxy reconstructions. We attribute this, in part, to the difficulty in defining the behavior of the Asian summer monsoon from any one variable, let alone single proxy records that are degraded by

TABLE 1. Multidecadal (>33 yr) correlations between the SASM IMI, the leading PCs of the three constituent fields of the SASM, and the leading PC of the precipitation field during full interval (850–1999) of simulation. Positive correlations that are statistically significant at the two-tailed $p = 0.01$ level ($p = 0.10$ level) are shown in boldface (italics). Annual correlations are provided in S1 of the online supplement.

	PC1 (SLP)	PC1 (U shear)	PC1 (V shear)	PC2 (V shear)	PC1 (precipitation)
PC1(SLP)	1				
PC1(U shear)	0.599	1			
PC1(V shear)	0.195	<i>0.209</i>	1		
PC2(V shear)	0.061	<i>0.292</i>	-0.065	1	
IMI	0.797	0.875	0.469	0.381	0.39

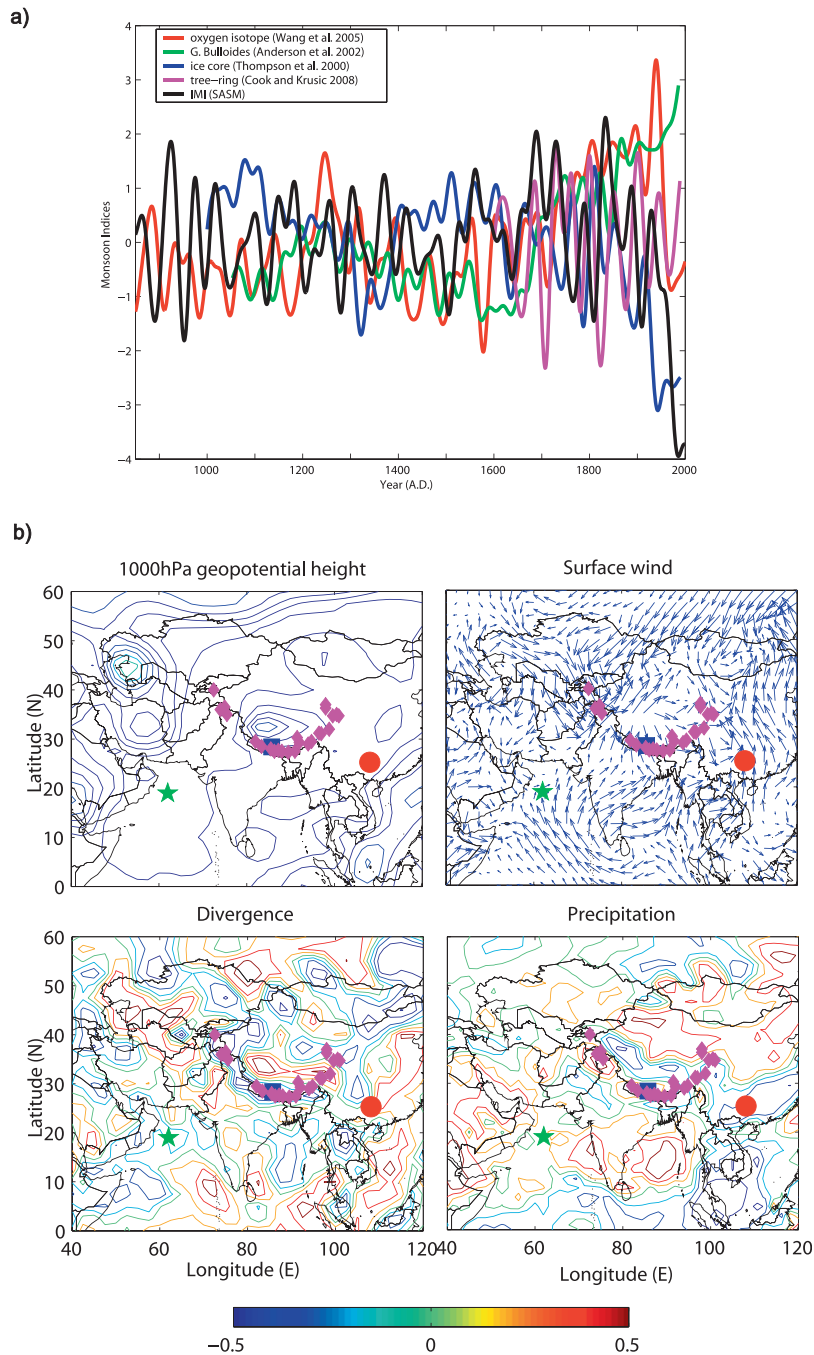


FIG. 4. Comparison between modeled and proxy reconstructed SASM histories. (a) Comparison of the simulated SASM IMI series with proxy reconstructions (smoothed on >33 -yr time scales and standardized to have unit variance) of the SASM. The reconstructions include a speleothem-based oxygen isotope reconstruction during 850–2000 from southwestern China reflecting humidity changes (Wang et al. 2005), an ocean sediment foraminifera-based reconstruction during 1053–1986 off the Arabian coast reflecting changes in upwelling (Anderson et al. 2002), Dasuopu ice core dust record during the interval 1000–1990 (Thompson et al. 2000), and Indian–Tibetan Plateau drought-sensitive tree-ring data during the interval 1600–1989 (Cook and Krusic 2009). (b) Maps of the proxy data locations against the modern annual correlation maps (based on NCEP reanalysis data) of SASM IMI against various meteorological fields: (top) (left) 1000-mb geopotential height and (right) surface winds.

TABLE 2. Multidecadal (>33 yr) correlations between SASM IMI and various proxy reconstructions of the ASM during the past 1000 yr. Positive correlations that are statistically significant at the one-tailed $p = 0.01$ level ($p = 0.1$ level) are shown in boldface (italics). Correlations are calculated both with and without twentieth-century data included to determine the robustness of relationships with respect to the large twentieth-century trend.

a. Full interval (1053–1986)					
	Wang	Anderson	Thompson	Cook	IMI
Wang	1				
Anderson	0.602	1			
Thompson	-0.364	-0.641	1		
Cook (1600–1986)	0.237	0.026	-0.081	1	
IMI	0.115	-0.214	<i>0.193</i>	-0.099	1
b. Premodern interval (1053–1900)					
	Wang	Anderson	Thompson	Cook	IMI
Wang	1				
Anderson	0.681	1			
Thompson	-0.310	-0.418	1		
Cook (1600–1900)	<i>0.205</i>	-0.034	-0.025	1	
IMI	0.151	<i>0.166</i>	-0.210	-0.046	1

potentially substantial nonclimate-related influences. It is difficult—given the present available evidence—to determine whether the model-based monsoon history or any of the proxy reconstructions provide a reliable indication of the true behavior of the Asian monsoon during the past 1000 yr.

5. Large-scale forcing of the Asian summer monsoon

We examined the relationships between the model-based SASM IMI and other large-scale climate metrics relevant for understanding the long-term evolution of the monsoon in the simulation.

The SASM IMI is observed to be broadly anti-correlated with both the Niño-3 index and Northern Hemisphere (NH) mean temperatures (Fig. 5). The substantial negative correlation ($r = -0.4$ at multidecadal time scales; see Table 3) between the monsoon index and the Niño-3 index is consistent with the established relationship between El Niño and monsoon failure at annual time scales evident in the modern record (see S1 of the online supplement). A statistically significant negative long-term relationship is also found between the SASM IMI and Northern Hemisphere mean annual temperatures (Table 3). This negative re-

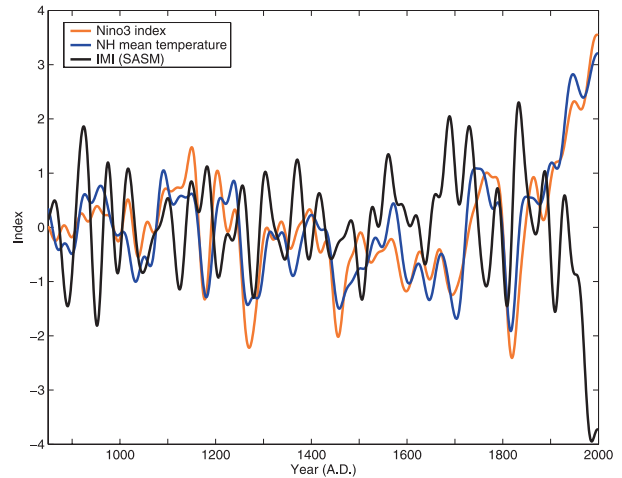


FIG. 5. Comparison of simulated SASM IMI (black), Niño-3, (orange), and NH mean temperature series (blue) during the interval 850–1999. All series have been smoothed to emphasize multidecadal time scales >33 yr.

lationship implies that in the simulation, warmer large-scale mean temperatures are associated with a weakened SASM. At least in the context of this simulation, this observation consequently argues against one possible mechanism that has been suggested for long-term forcing of the summer monsoon during the past millennium (Anderson et al. 2002), namely, that warmer large-scale mean temperatures, by decreasing the extent and duration of boreal spring Eurasian snow cover, might favor a stronger SASM. Such a relationship, first speculated by Blanford (1884), would imply a positive relationship rather than the negative relationship that is observed between NH mean temperature and SASM strength in our simulation. Fasullo (2004) recently examined the Blanford (1884) hypothesis using a diverse set of Eurasian snow cover indices and concluded that such a relationship, while it may exist in modern observations, is likely to be overwhelmed by other influences—for example, ENSO influences on the SASM. This conclusion is consistent with our findings. Applying each of the five different Eurasian spring snow cover index definitions used by Fasullo (2004) to the model, we found a significant and substantial negative multidecadal relationship between NH annual mean temperature and Eurasian spring snow cover (-0.6 to -0.76 , depending on the snow cover index; see section S1 of the online

←

FIG. 4. (Continued) and (bottom) (left) surface divergence and (right) precipitation. Proxy locations are denoted by a red circle for Wang et al. (2005), green star for Anderson et al. (2002), blue square for Thompson et al. (2000), and purple diamond for the spatial network of Cook and Krusic (2009).

TABLE 3. Multidecadal (>33 yr) correlations between the SASM IMI, NH mean temperature (NH), and Niño-3 series during full interval (850–1999) of the NCAR CSM1.4 simulation. Correlations that are statistically significant at the one-tailed $p = 0.01$ level ($p = 0.10$ level) are shown in boldface (italics). Annual correlations are provided in S1 of the online supplement.

Series	IMI	Niño-3	NH
IMI	1		
Niño-3	-0.44	1	
NH	-0.35	0.91	1

supplement) as expected. However, we found no evidence of the putative inverse relationship between SASM and snow cover at either the annual or multidecadal time scale. Indeed, at the multidecadal time scale, marginally significant *positive* correlations are observed ($r = 0.19$ – 0.29 , depending on the snow cover index), implying that positive anomalies in snow cover are in fact associated with a modestly stronger rather than weaker SASM. It is likely, therefore, that Eurasian snow cover is responding to, rather than causing, changes in the SASM in our simulation.

The negative relationship between Northern Hemisphere mean temperature and monsoon strength in the model appears to be associated, at least partially, with the Northern Hemisphere mean temperature and Niño-3 index being very tightly coupled in this simulation. The annual correlation $r = 0.72$ (see S1 of the online supplement) is considerably greater than that observed for the modern instrumental record ($r \sim 0.25$), and the correlation at multidecadal time scales ($r = 0.91$; see Table 3) approaches unity. Much of the closeness of this relationship is almost certainly due to the dynamical ENSO variability in the model being weak, leading temperatures in the Niño-3 region to respond somewhat passively to changes in radiative forcing, and thus to mirror the large-scale mean temperature changes themselves. The lack of any obvious dynamical response of ENSO to long-term radiative forcing contrasts with other analyses (e.g., Mann et al. 2005), and it represents one possible caveat in the interpretation of the present model results. Relationships between the monsoon index and changes in radiative forcing are investigated next.

6. External radiative forcing of the Asian summer monsoon

Changes in solar output and explosive volcanic activity are generally considered to be the primary natural external forcings acting over the past millennium (see Jones and Mann 2004). Both are included as forcings in the NCAR CSM simulation analyzed here. Although

past modeling studies have investigated the relationships between these natural forcings and ENSO (Mann et al. 2005) or the North Atlantic Oscillation–northern annular mode (Shindell et al. 2003) during the past millennium, no modeling studies to our knowledge have analyzed relationships between these forcings and the Asian summer monsoon during this time frame.

On a physical basis, we might expect solar output changes to be positively correlated with changes in the intensity of the SASM, since the differential summer land/ocean heating that drives the SASM is, of course, proportional to the magnitude of mean incoming solar insolation. However, we instead find a weak (albeit statistically insignificant) *negative* correlation between the SASM IMI and solar forcing at multidecadal time scales (Fig. 6a; Table 4). The absence of any positive relationship is consistent with the very weak nature of the associated radiative forcing ($\sim 0.1 \text{ W m}^{-2}$), which is likely overwhelmed by the intrinsic climate noise on multidecadal time scales. The negative relationship that is instead observed is likely related to factors discussed above. In the absence of a substantial direct radiatively forced response, the main influence of a positive radiative forcing is indirect. Positive forcing in this simulation leads to a more El Niño–like state in the tropical Pacific which, in turn, leads to a weakened SASM.

The real world situation appears to be quite different (Fig. 6b; Table 4). For three of the four proxy monsoon reconstructions discussed above, a sizeable and significant positive correlation with solar forcing ($r = 0.34$ – 0.37) is observed, rather than the weak negative relationship observed in the simulation. A plausible explanation is the aforementioned lack of any apparent dynamical tropical Pacific ocean–atmosphere response to radiative forcing in the simulation. Modeling evidence from Mann et al. (2005) suggests a significant El Niño–like (La Niña–like) dynamical response to negative (positive) solar radiative forcing during the past 1000 yr. Since El Niño is, in turn, associated with a weaker SASM, this dynamical response provides an additional mechanism by which a positive (negative) solar forcing anomaly should lead to an increase (decrease) in the strength of the SASM. That this mechanism appears active in the real world (e.g., Adams et al. 2003; Mann et al. 2005) but is not present in the simulation analyzed here, would provide a plausible explanation for why the statistically significant positive relationship apparent between solar forcing and the SASM is not reproduced in the simulation analyzed.

We then considered the effects of radiative forcing by explosive volcanism. Volcanic forcing yields far larger (negative), albeit short-lived, radiative forcing than does solar forcing during a time frame of several years.

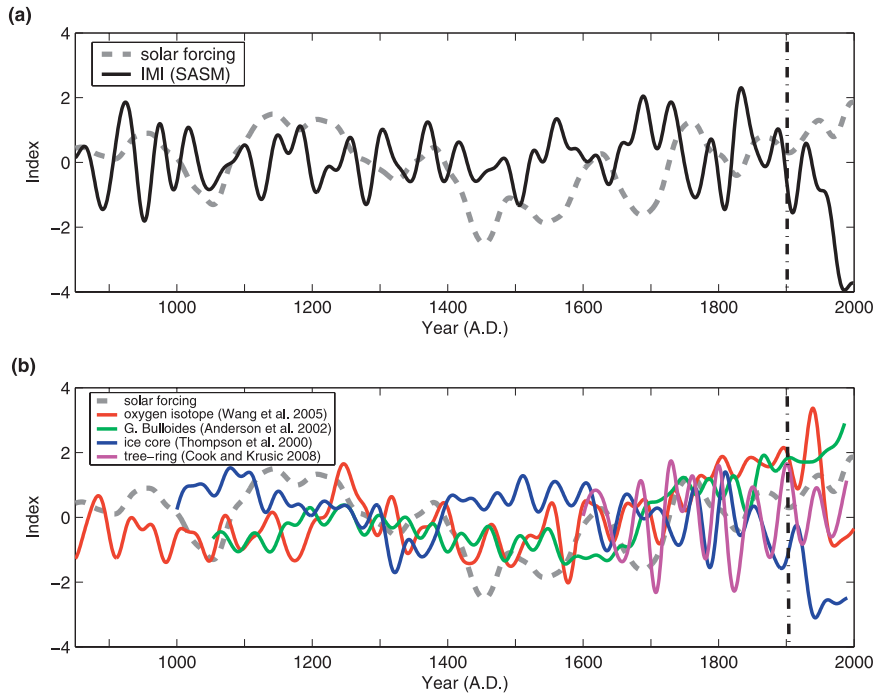


FIG. 6. Comparison of simulated SASM IMI series with solar radiative forcing. (a) Comparison of NCAR model monsoon index (black) with solar radiative forcing (dashed line) during the interval 850–1999. (b) Comparison of proxy monsoon reconstructions (Wang et al. 2005: red; Anderson et al. 2002: green; Thompson et al. 2000: blue; and Cook and Krusic 2009, manuscript submitted to *The Paleobotanist*: purple) with solar radiative forcing (dashed line). All series have been smoothed to emphasize multidecadal time scales >33 yr.

A number of volcanic eruptions over the past millennium (1150 yr to be precise) exceed -4 W m^{-2} in their surface radiative forcing. We might, therefore, expect a more readily discernible monsoon response to volcanic forcing in the simulation. Like anthropogenic aerosol forcing, we expect a negative relationship with the monsoon, with large eruptions reducing the differential summer land/ocean heating as a result of the lowered received surface insolation. Indeed, there is a notable qualitative correspondence between periods of large explosive volcanic activity and negative anomalies in the monsoon index—for example, in the late thirteenth, mid-fifteenth, seventeenth, and early nineteenth centuries (Fig. 7a).

We investigated the relationship with volcanic forcing quantitatively using “superposed epoch analysis” (SEA) to examine the composite behavior of the SASM IMI preceding, during, and following the year associated with a significant volcanic radiative forcing. As in the study of Mann et al. (2005) that examined the composite ENSO response to explosive volcanism in a modeling framework, we examined the composite response for both a smaller group (six) of the largest (negative radiative forcing exceeding -4 W m^{-2}) eruptions (Fig. 7b; composite includes eruptions occurring in 1177, 1258,

1278, 1452, 1809, and 1815) and a larger group (13) of eruptions with a lower magnitude threshold (negative radiative forcing exceeding -2 W m^{-2}) eruptions (Fig. 7c; composite includes eruptions occurring in the years

TABLE 4. Correlations with solar forcing. (a) Correlations between solar forcing, SASM IMI, NH mean temperature (NH), and Niño-3 series during the interval 850–1900 of simulation after smoothing at multidecadal (>33 yr) time scales. (b) Correlations of each of the three proxy monsoon reconstructions discussed in text with solar forcing at multidecadal (>33 yr) time scales during the interval 1053–1900. Positive correlations that are statistically significant at the one-tailed $p = 0.01$ level ($p = 0.10$ level) are shown in boldface (italics). The twentieth century has been eliminated, since anthropogenic forcing overwhelms the natural forced responses of interest after the nineteenth century.

	a.			
	IMI	NH	Niño-3	
Solar forcing (850–1900)	-0.093	0.548	0.560	
Reconstruction Solar forcing (1053–1900)	b.			
	Wang	Anderson	Cook (1600–1900)	Thompson
	0.355	0.365	0.336	-0.184

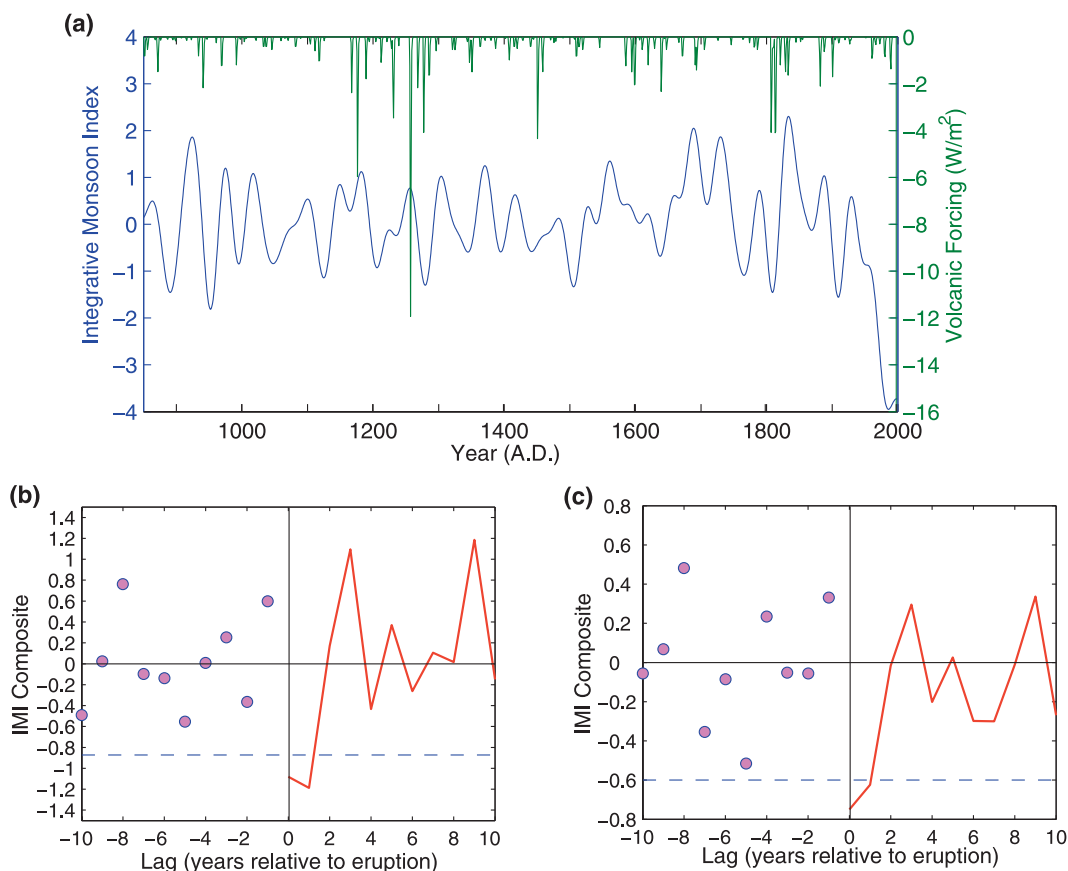


FIG. 7. Comparison of simulated SASM IMI series with volcanic forcing. (a) Comparison of the volcanic forcing time series (green) and SASM IMI (blue, smoothed to emphasize time scales >33 yr) during 850–1999. Shown also are SEA results based on composites of the (b) 6 volcanic events exceeding -4 W m^{-2} and (c) 13 volcanic forcing events exceeding -2 W m^{-2} during the period 850–1999. One-sided (negative) $p = 0.025$ significance levels for (b) and (c) are shown by horizontal dashed curves, estimated as two standard deviations of preeruption composite series below zero. Year 0 represents the year of the radiative forcing anomaly (which, depending on the seasonal timing of the eruption, may lag the year of the eruption by one year).

941, 1168, 1177, 1232, 1258, 1269, 1278, 1452, 1600, 1641, 1809, 1815, and 1884). In both cases, a highly significant ($p \ll 0.025$) negative response in the monsoon index is seen in both the year associated with the negative radiative forcing anomaly (year “0” in the SEA) as well as the following year (year “1”). Unfortunately, because the proxy SASM reconstructions discussed earlier are (with one exception) not annually resolved, it is not possible to perform a parallel analysis of volcanic forcing impacts using these records.

It should be noted that the monsoon response in the NCAR CSM1.4 simulation to volcanic forcing, like the response to solar forcing discussed above, might not include certain important dynamical responses that have the potential to increase the amplitude of the response. Proxy evidence from Adams et al. (2003) and modeling evidence from Mann et al. (2005) indicate a tendency for a short-term El Niño–like response to

explosive tropical volcanic forcing, a response that is not reproduced in the CSM simulation. As El Niños favor a weakened SASM, this effect should further amplify the weakening of the monsoon in response to volcanic forcing, beyond what is observed in the simulation.

7. Conclusions

Using a recently developed approach for defining a robust measure of the ASM, we have focused on the behavior of the South Asian component, the SASM, in a simulation of the climate of the past millennium forced with estimated natural and anthropogenic radiative forcing. There are several important implications of the current study for our understanding of long-term changes in the Asian summer monsoon. In the context of the model simulation we have analyzed, certain mechanisms—for example, warmer large-scale temperatures favoring

decreased Eurasian snow cover and, therefore, a stronger monsoon—are inconsistent with the observed relationships, that is, in this case, with the observed negative long-term relationship between SASM strength and Northern Hemisphere mean temperature. Another important finding is that a solar-forced signal in long-term SASM behavior appears likely to be undetectable given the estimated amplitude of solar radiative forcing, in the absence of amplifying dynamical mechanisms not present in the simulation we have analyzed. That such a signal does, nonetheless, appear to exist in the real world arguably provides, therefore, some independent evidence for the importance of such mechanisms, in particular, a dynamical response of ENSO to radiative forcing changes, in the real world. Our analysis of the model response to explosive volcanism, by contrast, indicates a clearly detectable signal, which is associated with a short-term decrease in the strength of the SASM in response to the large negative volcanic aerosol radiative forcing. While such a signal should be detectable in principle, the lack of annual resolution in currently available proxy reconstructions of the long-term behavior of the SASM limits parallel analyses of the observations at present. Possible dynamical responses of ENSO to volcanic radiative forcing described in previous studies, which are absent in the simulation analyzed here, would likely enhance rather than diminish the response of the monsoon to volcanic radiative forcing.

Acknowledgments. M. E. M. and F. F. gratefully acknowledge support from the ATM program of the National Science Foundation (Grant ATM-0542356) and C. M. A. for support through the National Center for Atmospheric Research WCIAS program. We thank both Lonnie Thompson and Ed Cook for providing the proxy data compared in the study. The National Center for Atmospheric Research is sponsored by the National Science Foundation and is operated by the University Corporation for Atmospheric Research.

REFERENCES

- Adams, J. B., M. E. Mann, and C. M. Ammann, 2003: Proxy evidence for an El Niño-like response to volcanic forcing. *Nature*, **426**, 274–278.
- Ammann, C. M., F. Joos, D. S. Schimel, B. L. Otto-Bliesner, and R. A. Tomas, 2007: Solar influence on climate during the past millennium: Results from transient simulations with the NCAR Climate System Model. *Proc. Natl. Acad. Sci. USA*, **104**, 3713–3718.
- Anderson, D. M., J. T. Overpeck, and A. K. Gupta, 2002: Increase in the Asian southwest monsoon during the past four centuries. *Science*, **297**, 596–599.
- Barnett, T. P., L. Dümenil, U. Schlese, E. Roeckner, and M. Latif, 1989: The effect of Eurasian snow cover on regional and global climate variations. *J. Atmos. Sci.*, **46**, 661–686.
- Blanford, H. F., 1884: On the connection of the Himalaya snowfall with dry winds and seasons of drought in India. *Proc. Roy. Soc. London*, **37**, 3–22.
- Boville, B. A., and P. R. Gent, 1998: The NCAR Climate System Model, version one. *J. Climate*, **11**, 1115–1130.
- , J. T. Kiehl, P. J. Rasch, and F. O. Bryan, 2001: Improvements to the NCAR CSM-1 for transient climate simulations. *J. Climate*, **14**, 164–179.
- Cook, E. R., and P. J. Krusic, 2009: Experimental reconstructions of large-scale summer monsoon drought over India and the Tibetan Plateau using tree rings from ‘High Asia.’ *Paleobotanist*, in press.
- Fasullo, J., 2004: A stratified diagnosis of the Indian Monsoon—Eurasian snow cover relationship. *J. Climate*, **17**, 1110–1122.
- Goswami, B. N., V. Krishnamurthy, and H. Annamalai, 1999: A broad-scale circulation index for the interannual variability of the Indian summer monsoon. *Quart. J. Roy. Meteor. Soc.*, **125**, 611–633.
- Grove, R. H., 1998: Global impact of the 1789–93 El Niño. *Nature*, **393**, 318–319.
- Hurrell, J. W., and K. E. Trenberth, 1998: Difficulties in obtaining reliable temperature trends: Reconciling the surface and satellite microwave sounding unit records. *J. Climate*, **11**, 945–967.
- Jones, P. D., and M. E. Mann, 2004: Climate over past millennia. *Rev. Geophys.*, **42**, RG2002, doi:10.1029/2003RG000143.
- Kiehl, J. T., 1998: Simulation of the tropical Pacific warm pool with the NCAR Climate System Model. *J. Climate*, **11**, 1342–1355.
- Krishna Kumar, K., B. Rajagopalan, and M. A. Cane, 1999: On the weakening relationship between the Indian Monsoon and ENSO. *Science*, **284**, 2156–2159.
- , —, M. Hoerling, G. Bates, and M. A. Cane, 2006: Unraveling the mystery of monsoon failure during El Niño. *Science*, **314**, 115–119.
- Mann, M. E., 2004: On smoothing potentially non-stationary climate time series. *Geophys. Res. Lett.*, **31**, L07214, doi:10.1029/2004GL019569.
- , M. A. Cane, S. E. Zebiak, and A. Clement, 2005: Volcanic and solar forcing of the tropical Pacific over the past 1000 years. *J. Climate*, **18**, 447–456.
- Meehl, G. A., 1994: Coupled land–ocean–atmosphere processes and South Asian monsoon variability. *Science*, **266**, 263–267.
- , and J. M. Arblaster, 2003: Mechanisms for projected future changes in south Asian monsoon precipitation. *Climate Dyn.*, **21**, 659–675.
- , and Coauthors, 2007: Global climate projections. *Climate Change 2007: The Physical Science Basis*, S. Solomon et al., Eds., Cambridge University Press, 747–846.
- Nigam, S., 1994: On the dynamical basis for the Asian summer monsoon rainfall–El Niño relationship. *J. Climate*, **7**, 1750–1770.
- Otto-Bliesner, B. L., and E. C. Brady, 2001: Tropical Pacific variability in the NCAR Climate System Model. *J. Climate*, **14**, 3587–3607.
- Parthasarathy, B., R. R. Kumar, and D. R. Kothawale, 1992: Indian summer monsoon rainfall indices, 1871–1990. *Meteor. Mag.*, **121**, 174–186.
- Shindell, D. T., G. A. Schmidt, R. L. Miller, and M. E. Mann, 2003: Volcanic and solar forcing of climate change during the pre-industrial era. *J. Climate*, **16**, 4094–4107.
- Thompson, L. G., T. Yao, E. Mosely-Thompson, M. E. Davis, K. A. Henderson, and P.-N. Lin, 2000: A high-resolution millennial

- record of the south Asian monsoon from Himalayan ice cores. *Science*, **289**, 1916–1919.
- Wang, Y., and Coauthors, 2005: The Holocene Asian monsoon: Links to solar changes and North Atlantic climate. *Science*, **308**, 854–857.
- Webster, P. J., and S. Yang, 1992: Monsoon and ENSO: Selectively interactive systems. *Quart. J. Roy. Meteor. Soc.*, **118**, 877–926.
- , V. O. Magana, T. N. Palmer, J. Shukla, R. A. Tomas, M. Yanai, and T. Yasunari, 1998: Monsoons: Processes, predictability, and the prospects for prediction. *J. Geophys. Res.*, **103**, 14 451–14 510.
- Wolter, K., and M. S. Timlin, 1993: Monitoring ENSO in COADS with a seasonally adjusted principal component index. *Proc. 17th Climate Diagnostics Workshop*, Norman, OK, NOAA/NMC/CAC, 52–57.